Corrosion Science 140 (2018) 73–78

Contents lists available at ScienceDirect

Corrosion Science

journal homepage: www.elsevier.com/locate/corsci

Corrosion behaviour of electrodeposited Zn-Cr alloy coatings

V. Chakarova[a], Tz. Boiadjieva-Scherzer[b,*], D. Kovacheva[c], H. Kronberger[d], M. Monev[a]

[a] Institute of Physical Chemistry, Bulgarian Academy of Sciences, Acad G. Bonchev Str., Bl.11, Sofia, 1113, Bulgaria
[b] Centre of Electrochemical Surface Technology GmbH, Viktor-Kaplan-Straße 2, 2700, Wiener Neustadt, Austria
[c] Institute of General and Inorganic Chemistry, Bulgarian Academy of Sciences, Acad G. Bonchev Str., Bl.11, Sofia, 1113, Bulgaria
[d] TU-Vienna, Institute for Chemical Technology and Analytics, Getreidemarkt 9/164ec, A-1060, Vienna, Austria

ARTICLE INFO

Keywords:
Electrodeposited Zn-Cr alloy
AAA
SEM
XRD
Corrosion
Anodic dissolution

ABSTRACT

Electrodeposited Zn-Cr alloy coatings show a high potential in protecting steel from corrosion. Investigations in sulphate solutions by electrochemical and analytical methods demonstrate low corrosion of the coatings in pH 4–12 range. Significant dissolution is observed at pH < 4.0, where the alloys dissolve with a higher rate than Zn. The corrosion performance is related to dissolution of the corrosion protective film and the lower hydrogen overvoltage on the alloys than that on Zn. After corrosion of Zn-10.4%Cr the phase composition retains as the parameter (a) of Γ-(Zn,Cr) phase does not change, whereas the parameter (c) of δ-(Zn,Cr) phase decreases.

1. Introduction

A number of studies demonstrate better corrosion protective properties of electrodeposited Zn-Cr alloy coatings on steel in comparison to Zn coatings [1–6] and the electrodeposition of Zn-Cr has been optimized for high speed plating on steel strips for car body application in the automotive industry [7,8]. Excellent results in corrosion protection were obtained with alloy coatings containing 3–7 mass % Cr.

Of scientific and practical interest is the corrosion resistance of the alloys themselves because of several reasons. In the range of pH 6–12 the rate of Zn corrosion is relatively low and proceeds predominantly with oxygen depolarization [9]. The Zn surface is commonly covered by a film consisting of Zn oxide as a main constituent and Zn hydroxide, present in different amounts (in case of absence of species with which Zn may form compounds of low solubility) [10]. The film has the effect of inhibiting the dissolution. At pH below and above the neutral range, Zn corrodes with a high rate, due to its amphoteric character and high solubility of the corrosion products. At low pH Zn dissolves to give Zn^{2+} with hydrogen depolarization, because of the high hydrogen ion concentration. At high pH values the Zn dissolution is enhanced because of the formation of soluble bizincate or zincate ions ($HZnO_2^-$ and ZnO_2^{2-}). The dissolution of Zn can follow different mechanisms; generally, under steady-state conditions at low pH values (up to 3) the dissolution of Zn is kinetically controlled by the charge transfer reaction, whereas at high pH (> 12) it is controlled by diffusion of $HZnO_2^-$ or ZnO_2^{2-} away from the surface [10]. Referring to the standard electrode potentials Cr is supposed to perform similarly to Zn in corrosion-chemical aspect. The fact that Cr behaves almost like a noble metal is due to a surface passivation which results from the formation of dense and largely insoluble surface layers of Cr-oxides even by an insignificant oxidizing impact. This is the reason for the high corrosion resistance of Cr in atmospheric environment and in most chemicals (except hydrochloric acid and hot sulfuric acid). The easy passivation and thermal stability of Cr determine its use as an alloying component for different metals.

As the Zn-based protective layers are exposed during production and application to media largely differing in their pH values the electrochemical behaviour of Zn-Cr in regard to the acidity of the corrosion medium is of particular interest. The electrodeposition of the Zn-Cr alloy coatings is carried out from acidic sulfate electrolytes with pH in the range of 1–4, most often pH of 2 [11]. Hence, an interruption of the plating procedure would expose the deposited layer to the corrosive electrolyte causing re-dissolution at rates which may be influenced by the composition of the alloys. Moreover, in order to obtain the final product, the electrogalvanized Zn-Cr steel sheet undergoes further treatments in acidic or alkaline solutions for application of additional layers (for example phosphate layer). In the present work, the corrosion behaviour of Zn-Cr alloy coatings with different Cr content in sulphate solutions was investigated in a wide range of pH.

2. Experimental

Zn-Cr alloy coatings were electrodeposited from an electrolyte, containing 40 g l^{-1} Zn, 15 g l^{-1} Cr (added as sulphates) and PEG 6000

* Corresponding author.
E-mail address: tzvetanka.boiadjieva@cest.at (T. Boiadjieva-Scherzer).

https://doi.org/10.1016/j.corsci.2018.06.019
Received 17 July 2017; Received in revised form 8 June 2018; Accepted 15 June 2018
Available online 19 June 2018
0010-938X/

($1\ g\ l^{-1}$), pH 2.0, adjusted with sulphuric acid, in a 20 l flow cell, flow rate $4\ m\ s^{-1}$, electrolyte temperature 40 °C onto mild steel substrates with dimensions 115 × 85 mm. At the above conditions and current density of $80\ A\ dm^{-2}$ alloy coatings with an average Cr content of 3.6 mass % and average thickness of 2.5, 5 and 7 μm were obtained at 11, 22, and 30 s deposition time, respectively. Zn-10.4%Cr coatings were deposited at a current density of $120\ A\ dm^{-2}$ with an average thickness of 2.5, 5 and 7 μm by varying the deposition time – 8, 14 and 25 s, respectively. Zn coatings with a thickness of 2.5, 5 and 7 μm were electrodeposited from an electrolyte without Cr(III) and PEG. All chemicals used were of analytical grade.

The Cr content in the alloy coatings and the coatings thickness were determined by using X-ray fluorescence analysis (XRFA) (Fischerscope XDL-B, Software WinFTM 6.09). The elemental composition was also measured by Energy Dispersive X-Ray (EDX) spectrometer supported with Genesis software (USA).

Open circuit potential (OCP) transients were plotted in 0.5 M Na_2SO_4 solution with pH 5.9. Potentiodynamic polarization with a scan rate of $1\ mV\ s^{-1}$ was applied in order to study the anodic dissolution of the coatings. The investigations were performed in a three-electrode cell having a volume of 50 ml, a reference Hg/Hg_2SO_4 electrode, a working electrode with a surface area of $0.2\ cm^2$ and a Pt counter electrode. All electrochemical experiments were carried out using a potentiostat/galvanostat model 263 A (EG&G Princeton Applied Research, USA) and software SoftCorr II. The polarization resistance (R_P) is calculated from data collected during the potentiodynamic polarization.

The corrosion studies were carried out in 0.5 M Na_2SO_4 solution at a temperature of 25 °C. The pH of the solution was varied in the range 1.0–13.3 by addition of H_2SO_4 or NaOH. Samples with a working surface area of $0.785\ cm^2$ were immersed in the corresponding solutions and after each 1 min stay were weighed for calculation of the weight loss. Sample solutions were examined by atomic-absorption analysis (AAA) and the dissolved amounts of Zn and Cr were determined. The changes of the thickness of the coatings and of the Cr content in the alloys were followed by means of XRFA and EDX.

The surface morphology was analyzed by XL 30 environmental scanning electron microscope (ESEM) with field emission gun FEI Co., Netherlands. Three-dimensional (3D) area analyses, directly from the stereoscopic images of the specimen surface were carried out using MeX software from Alicona A. The surface morphology before and after corrosion treatment was analyzed by SEM, JEOL JSM 733, Japan, as well.

X-ray powder diffraction patterns were collected within the range from 10 to 100° 2θ with a constant step 0.02° 2θ on Bruker D8 Advance diffractometer with Cu K_α radiation and LynxEye detector. Unit cell parameters were determined with the Topas-4.2 software package using the fundamental parameters peak shape description including appropriate corrections for the instrumental broadening and diffractometer geometry.

3. Results and discussion

3.1. Stationary measurements

In 0.5 M Na_2SO_4, pH 5.9 the OCP of the Zn coating is in about 400 mV more negative than that of steel (Fig. 1). The OCP of the Zn-Cr alloy coating with 10.4 mass % Cr is in about 150 mV more positive than Zn, but still sufficiently negative to the steel substrate to provide sacrificial protection. The increase of the thickness of the Zn coating is reflected in a slight shift of the potential in negative direction, indicating influence of the steel substrate for the thinner coatings (Fig. 2). The thin Zn layer probably does not densely cover the substrate due to the rough structure (large hexagonal crystallites) of Zn [12].

The effect of the thickness for the Zn-Cr alloy coatings is insignificant. In contrast, the effect of the Cr content in the alloy is stronger – the higher the Cr content is, the more positive the steady state potential is (Fig. 1). Further investigations were carried out mainly with Zn and alloy coatings having a thickness of 7 μm.

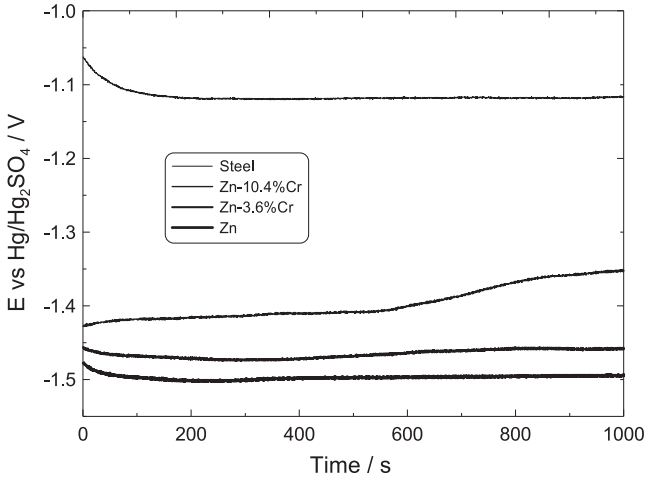

Fig. 1. OCP-time relation obtained for steel, Zn and Zn-Cr coatings with an average thickness of 7 μm in 0.5 M Na_2SO_4 solution, pH 5.9.

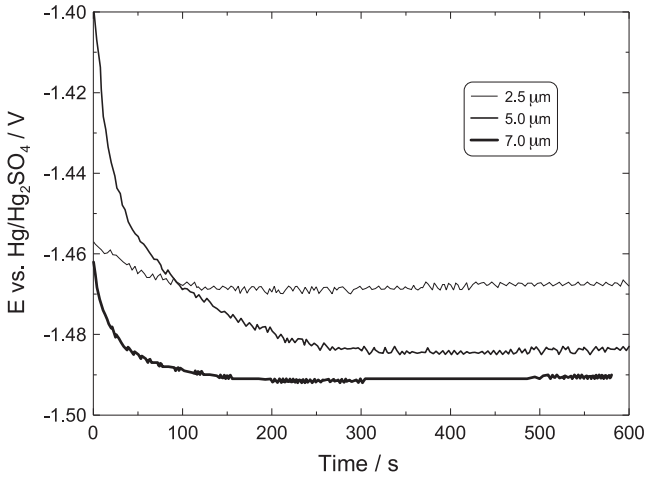

Fig. 2. OCP-time relation obtained for Zn coatings with different thickness in 0.5 M Na_2SO_4 solution, pH 5.9.

The differences between the surface states of the Zn and Zn-Cr alloy coatings are also reflected by the time for reaching steady state potential. The potential-time curves for the alloys show a tendency for change of the corrosion potential with time, since corrosion of Zn and enrichment of the surface in Cr takes place. The effect is more pronounced for the alloys with higher Cr content (10.4 mass % Cr) (Fig. 1). A corrosion test by total immersion of Zn and Zn-14%Cr specimens into corrosive media (0.5 M Na_2SO_4, pH 5.4) showed that the time of appearance of red rust for the alloy coating is 100 h longer than that for Zn coating [13].

3.2. Anodic potentiodynamic polarization curves

The effect of the alloying of Zn with Cr on the dissolution behaviour is demonstrated by the potentiodynamic polarization curves (Fig. 3). Following a wide area of active dissolution the steel passivates at a potential of about 0.2 V. Two anodic maxima are observed on the potentiodynamic curves for the Zn and Zn-Cr alloy coatings. Subsequently, Zn and Zn-Cr alloy samples were polarized to a potential after the first anodic maximum and the surfaces were analyzed by XRFA and EDX. The XRFA analysis showed traces of Zn on the surface of the Zn

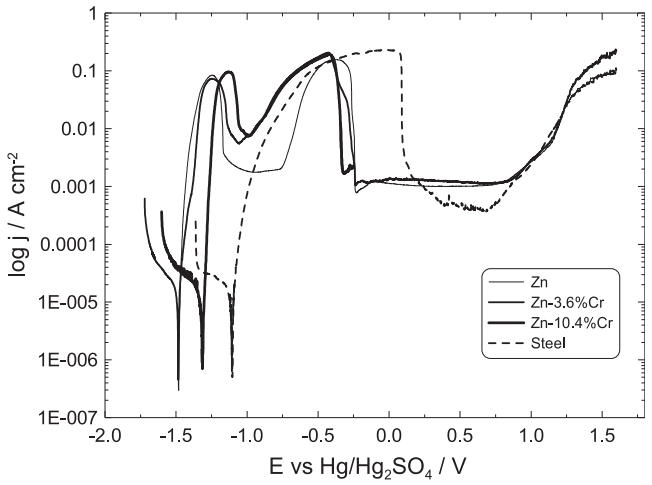

Fig. 3. Potentiodynamic polarization curves for steel, Zn and Zn-Cr alloy coatings with different Cr content in 0.5 M Na_2SO_4, pH 5.9.

coated sample. By AAA only Zn^{2+} ions were registered in the solution. The rate of active dissolution and the maximum values of current density of active dissolution for Zn and Zn-3.6%Cr practically coincide, while the active dissolution range for the Zn-10.4%Cr is shifted to less negative potentials with about 100 mV. Despite of the different initial ("as plated") composition of the alloy coatings, the Cr content in the remaining layer after the first maximum reaches 28–38 mass % implying preferential Zn dissolution, in consistency with data in [14]. It should be noted, that the values for the Cr content are informative, but not absolute since the coatings' thickness is strongly reduced to 0.4 and 1.2 µm, respectively. SEM images of "as deposited" Zn-3.6%Cr and Zn-10.4%Cr samples and after potentiodynamic polarization to a potential after the first anodic maximum are presented in Fig. 4. Occasionally, dendrites on the surface of the as deposited Zn-3.6%Cr coatings were observed. Aiming at a better visualization, three-dimensional area analyses, directly from the stereoscopic images were performed and 3D SEM images were build (Fig. 4a). However, no "marks" from the dendrites could be distinguished on the surface after the anodic treatment (Fig. 4b). Furthermore, the 2D SEM images show irregular corrosion of the Zn-Cr coatings (Fig. 4b).

For the Zn coated sample the second anodic maximum is related to dissolution of steel from the substrate. The second anodic maximum for the alloy coated samples is due to two processes. Dissolution of (Zn,Cr) phase [14] and dissolution of the steel substrate trough the discontinuous alloy coating. As a consequence, the otherwise chemically stable, enriched in Cr layer remains without a support. Undissolved particles mechanically disintegrate and shed from the surface. For all coated samples the passivation of the steel takes place at a more negative potential than that of non-treated steel. This could be related to presence of residuals from the coatings (Zn or Zn-Cr) on the steel surfaces during the passivation process. Moreover, a "print" of the deposition process on the steel surface and sub-surface caused by strong coating-substrate interaction, namely UPD Zn deposition on steel, possible Fe-Zn alloying is to consider.

The increase of the current at a potential of about 1 V is related to oxygen evolution on the electrode surfaces.

Results from elaboration of the potentiodynamic polarization curves are presented in Table 1.

The increase of the Cr content in the alloy results in a shift of the corrosion potential in a positive direction and an increase of the polarization resistance. No data about the corrosion currents are derived from the potentiodynamic curves. It is known that corrosion current is meaningful only for evaluating certain corrosion situations where the corrosion is essentially uniform over the whole surface area [10]. The SEM images in Fig. 4b validate that attempts in determining corrosion

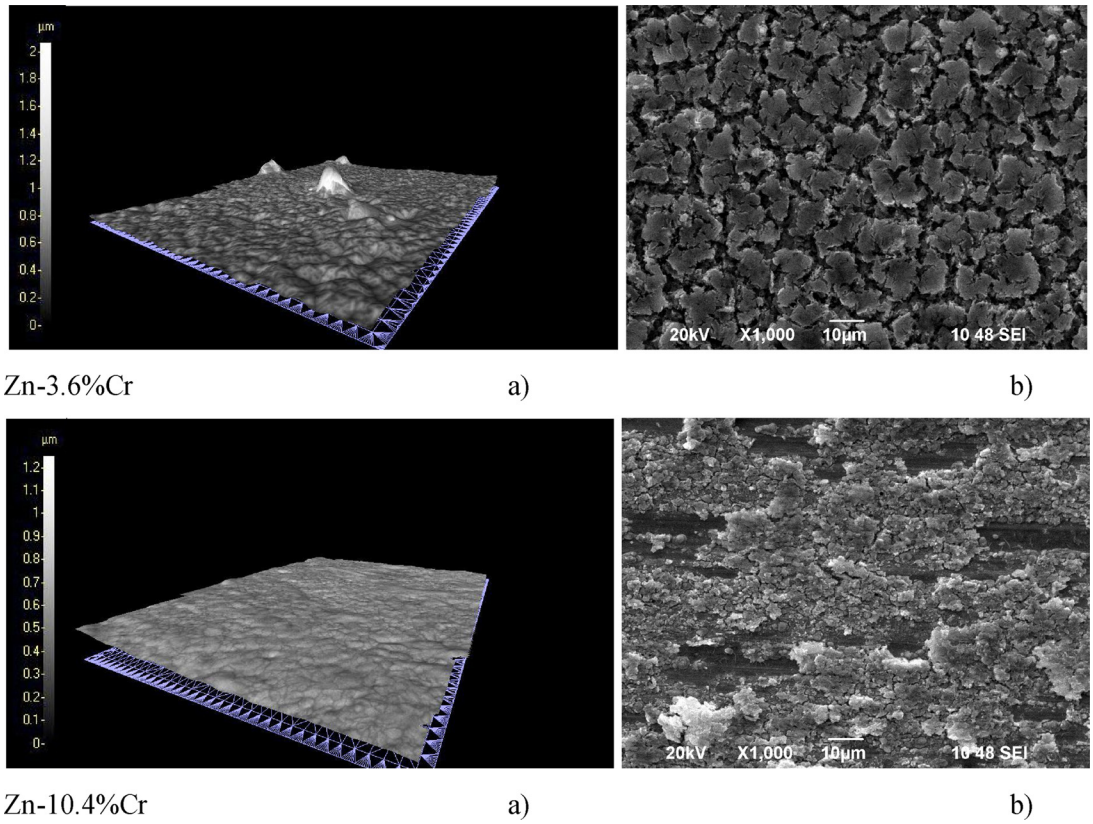

Fig. 4. SEM images of "as deposited" Zn-3.6%Cr and Zn-10.4%Cr samples (3D SEM) (a) and after potentiodynamic polarization to a potential after the first anodic maximum (2D SEM) (b).

Table 1
Effect of the Cr content in the alloy coating on the corrosion potential and polarization resistance in 0.5 M Na_2SO_4, pH 5.9.

	E_{corr} / V	R_P / kΩ
Zn	−1.49	0.4
Zn-3.6%Cr	−1.43	3.4
Zn-10.4%Cr	−1.36	5.1

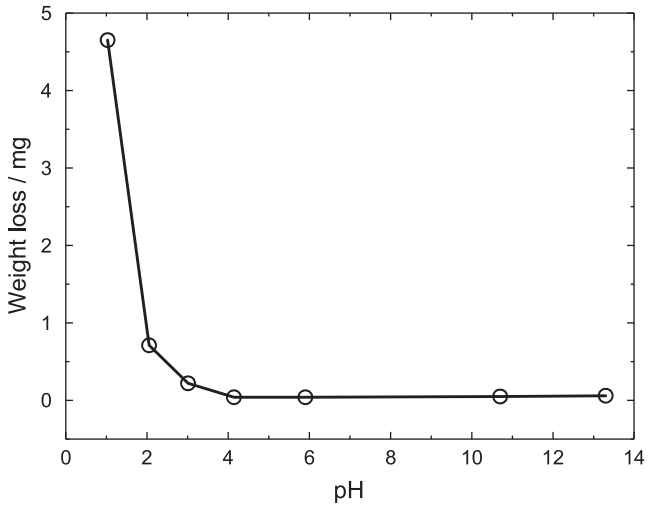

Fig. 5. Relationship between total weight loss for Zn-10.4%Cr after 3 min (three sequential exposures of 1 min each) immersion time and pH of the 0.5 M Na_2SO_4.

Table 2
Dissolution rate of Zn and Cr from Zn and Zn-Cr coated samples in 0.5 M Na_2SO_4 with pH 1.3. The amount of the dissolved Cr as a percentage of the total dissolved coating mass after 3 min immersion time is presented in brackets.

	Dissolution rate mg / min cm^2	
	Zn	Cr
Zn	0.13	–
Zn-3.6%Cr	0.45	0.013 (2.8 %)
Zn-10.4%Cr	1.04	0.115 (9.9 %)

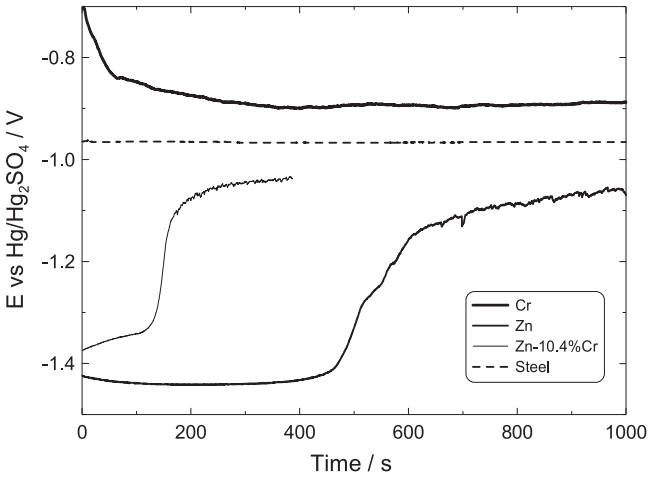

Fig. 6. OCP-time relation obtained for Zn, Cr and Zn-10.4%Cr coatings in 0.5 M Na_2SO_4, pH 1.0.

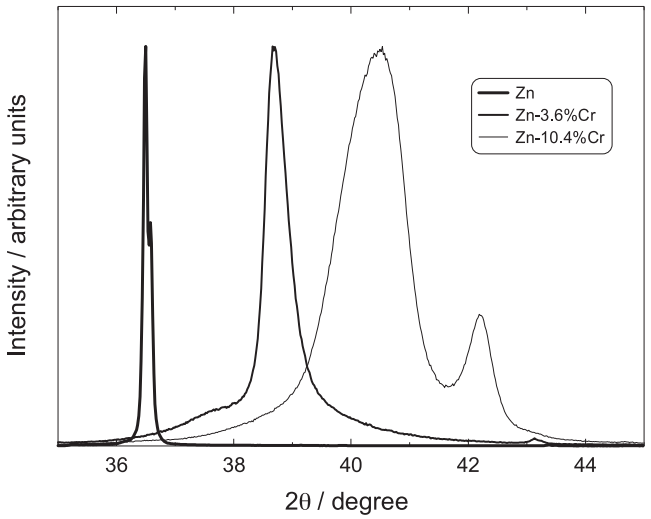

Fig. 7. Normalized XRD patterns for "as deposited" Zn and Zn-Cr alloy coatings with different Cr content.

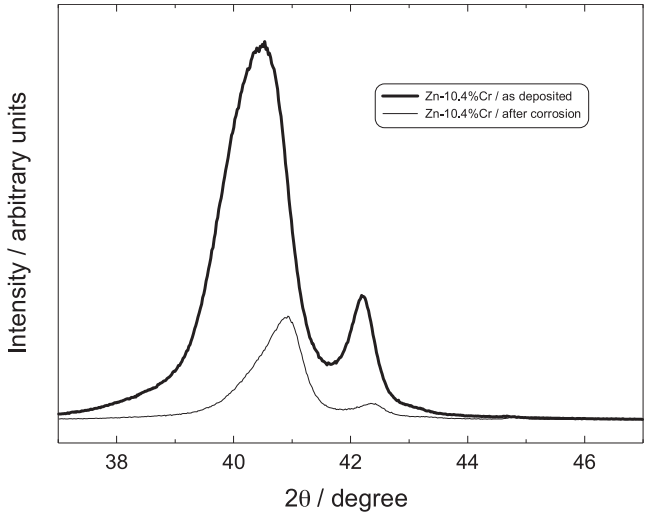

Fig. 8. XRD patterns for "as deposited" Zn-10.4%Cr alloy coating and after corrosion treatment of the coating for time duration of 3 min in 0.5 M Na_2SO_4, pH 1.3.

Table 3
Change of lattice parameters of the (Zn,Cr) phases of Zn-10.4%Cr alloy coating after 3 min immersion time in 0.5 M Na_2SO_4 with pH 1.3. The relative content of Γ-(Zn,Cr) phase is presented in brackets.

	δ-(Zn,Cr) phase		Γ-(Zn,Cr) phase
	a / Å	c / Å	a / Å
as deposited	2.789(2)	4.461(4)	3.024(4) (10 %)
after corrosion treatment	2.806(2)	4.437(2)	3.023(1) (6 %)

currents would result in large errors.

3.3. Effect of the acidity of the solution on the corrosion of the alloy coatings

Fig. 5 presents the effect of the acidity of the solution on the corrosion of Zn-10.4%Cr alloy coating, expressed by weight loss. The Zn-Cr alloys, as well Zn, corrode in the pH 4–12 range with a low rate. The dissolution rate significantly increases when the pH value is lower than 4. This could be related, along with other factors to the dependence between Cr dissolution and pH, according to the Pourbaix potential-pH

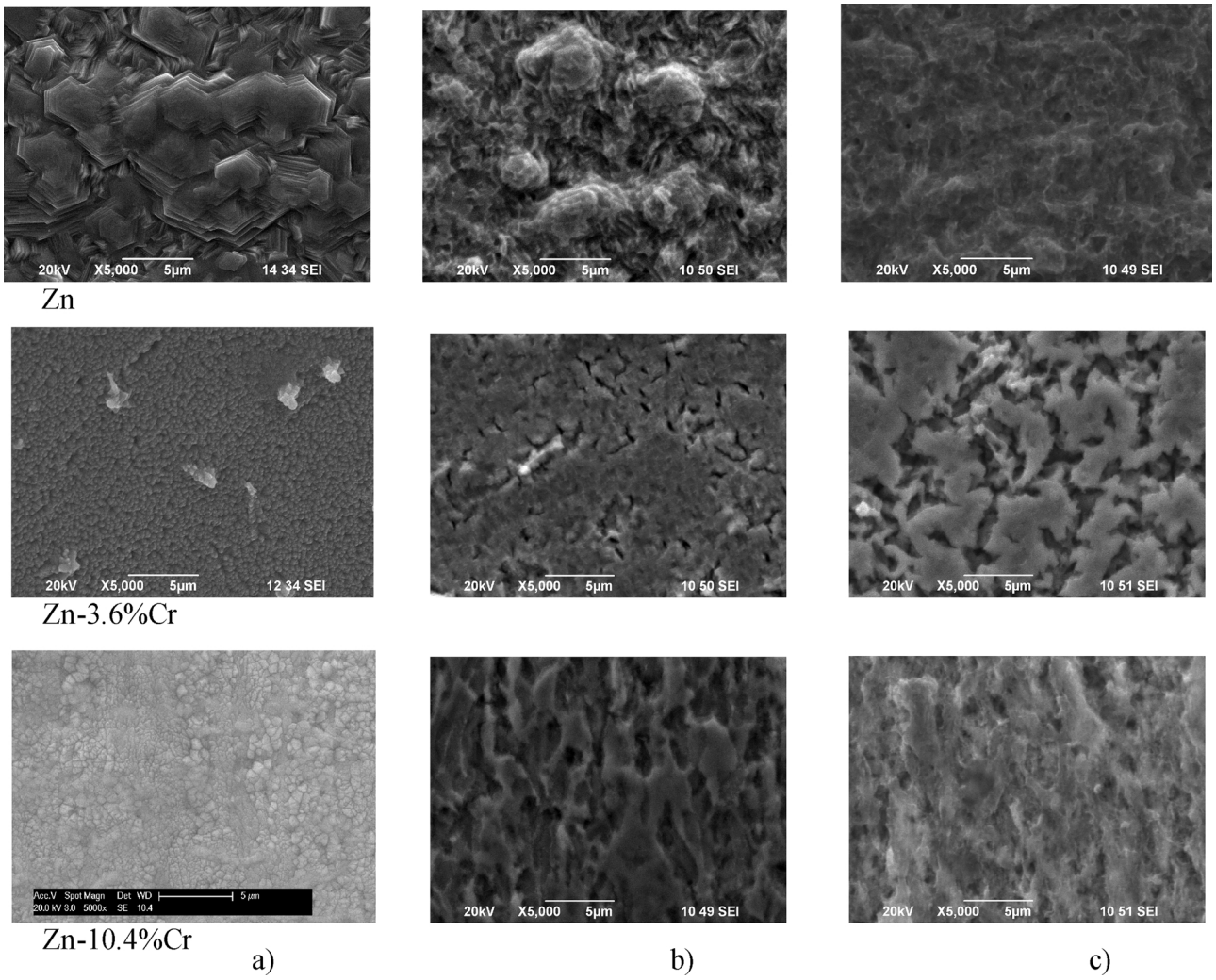

Fig. 9. SEM images of the surface of Zn and Zn-Cr alloy coatings with different Cr content – before (a) and after corrosion treatment for time duration of 1 min (b) and 3 min (c) in 0.5 M Na_2SO_4, pH 1.3.

equilibrium diagram for the Cr-H_2O system [15].

In order to compare the rate of dissolution of Zn-Cr alloys with different Cr content to that of Zn, a solution with pH of 1.3 was chosen. The dissolution rate was determined by AAA of solutions after corrosion of the respective specimens. Average values are presented in Table 2.

The alloy coatings dissolve with a considerably higher rate in comparison to that of Zn. With the increase of the Cr content in the alloy the dissolution rate increases. The dissolved amount of Cr is 2.8 and 9.9% from the overall dissolved mass of the corresponding coatings.

In Fig. 6 the potential transients for Zn and Zn-10.4%Cr coated samples (similar thickness of the coatings) in 0.5 M Na_2SO_4 with pH 1.0 are compared. The change of the potentials with time also indirectly illustrates a higher dissolution rate of the alloy. It is worth mentioning that the coatings' potentials shift towards the potential of the substrate due to the corrosion process, but stay negative to that of steel (results in consistency with Section 3.2. *Anodic potentiodynamic polarization*). The pure Cr coating does not dissolve under those conditions due to its passive state and remains more positive than the steel.

The higher dissolution rate of the alloys in comparison to Zn can be related to the combined effects of dissolution of the film of corrosion products on the alloys in acidic environment from one hand and the lower hydrogen overvoltage on the alloys than that on Zn, from another hand. The main constituents of a surface film formed on Zn-Cr alloys after deposition and contact with air are the Zn oxide/hydroxides [16,17]. The Zn-Cr coatings demonstrate corrosion protective properties in a wide range of pH (were further gradual formation and buildup of oxide/hydroxide film takes place), but not at low pH values. In acidic media not only the oxide/hydroxides are soluble, but also Zn and Cr are thermodynamically not stable, *i.e.* active corrosion takes place. Moreover, the contact of Cr with Zn ($E^{\circ}_{Zn(II)/Zn(0)} = -0.76$ V) in a corrosive medium decreases the potential to values below the redox potential of Cr(III)/Cr(II) ($E^{\circ}_{Cr(III)/Cr(II)} = -0.4$ V) which activates even passive Cr by reducing the passive layers. Partial or complete dissolution of the corrosion protective film exposes the Zn-Cr surface to the high concentration of hydrogen ions. It is well known, that in acidic environments the hydrogen evolution reaction (HER) represents the dominating counter reaction to metal dissolution. Consequently, the lower the hydrogen overvoltage is the higher the rate of the HER would be. Studies of the HER on Zn-Cr alloys showed that the hydrogen overvoltage on Zn-10.4%Cr alloy is more than 200 mV lower than that on Zn [12].

3.3.1. Phase composition

XRD patterns for the "as deposited" Zn and Zn-Cr alloy coatings are presented in Fig. 7. The Zn coating has hexagonal (hcp) lattice with unit cell parameters a = 2.667 Å and c = 4.945 Å. The alloy coating with 3.6 mass % Cr consist of non-equilibrium δ-(Zn,Cr) phase with hexagonal lattice, a = 2.691(6)Å and c = 4.84(1)Å, regarded as super-saturated solid solution of Cr in Zn matrix [11]. With increasing Cr

content (Zn-10.4%Cr) along with the δ-(Zn,Cr) phase (a = 2.789(2) Å and c = 4.461(4)Å), a cubic Γ-(Zn,Cr) phase (partially ordered limited solid solution) with a lattice parameter a = 3.024(4)Å is registered.

The XRD pattern of alloy coating Zn-10.4%Cr after corrosion in 0.5 M Na_2SO_4 with pH 1.3 at room temperature is shown in Fig. 8. Phase composition and unit cell parameters data are summarized in Table 3.

The unit cell parameter of the Γ-(Zn,Cr) phase actually does not change. A decrease of the parameter *(c)* of the δ-(Zn,Cr) is observed, which suggests higher dissolution rate of Zn. These findings are in agreement with the results from AAA of solutions after corrosion (Table 2). It has to be noted that the (002) diffraction line is wider in the low angle range (Fig. 8). Such type of asymmetry is an indication for a concentration gradient within the layer [18]. EDX investigations of a cross-section of "as deposited" Zn-10.4%Cr alloy coating showed a small increase of the Cr content from the interface zone towards the surface. Obviously, in the course of the corrosion process this gradient in the Cr distribution is enhanced.

3.3.2. *Morphology of the coatings*

The changes in the morphology of Zn and Zn-Cr alloy coatings caused by corrosion treatment were followed by using SEM (Fig. 9). The Zn dissolution starts at the edges of the characteristic hexagonal crystallites and advances towards uniformly corroded surface. The corrosion of the alloy with low Cr content is localized at the grain boundaries, which with the time progress widen, forming "a canyon-like" structure. The alloy with high Cr content corrodes irregularly and forms a porous structure.

4. Conclusions

The steady state potential of the electrodeposited Zn-Cr alloy coatings in neutral sulphate medium is about 150 mV more positive than that of Zn (in the boundary case of 10.4 mass % Cr) and it is still sufficiently negative compared to the steel substrate to provide sacrificial protection. The shift of the potential in positive direction increases in magnitude with increasing the Cr content in the alloy.

The Zn-Cr alloy coatings corrode at a low rate in sulphate solutions, in a wide range of pH. Significant dissolution is observed at pH below 4.0. The dissolution rate increases with the acidification of the solution and with the increase of the Cr content in the alloy. In the acidic range the Zn-Cr alloy dissolves with considerably higher rate than Zn. The corrosion of the alloys is non-uniform. The combined effects of partial or complete dissolution of the corrosion protective film at low pH values and the lower hydrogen overvoltage on the alloys determine the observed behaviour. After corrosion of Zn-10.4%Cr alloy coatings the residual layer consist of hcp δ-(Zn,Cr) and bcc Γ-(Zn,Cr) phases, detected also in the starting "as deposited" coatings. The unit cell parameter *(c)* of the δ-(Zn,Cr) phase decreases, indicating preferential corrosion of Zn from this phase; whereas the lattice structure of the Γ-(Zn,Cr) phase does not change.

Acknowledgement

These investigations were performed with the support of the Austrian Science Foundation FFG and the government of Lower Austria and Upper Austria in the frame of the COMET program. The authors acknowledge the financial support of Project BG051PO001-3.3.06-0038. The authors wish to thank voestalpine Stahl GmbH, Linz, Austria for providing samples used in the present investigations.

References

[1] T. Kanamaru, M. Nakayama, K. Araj, S. Suzuki, R. Naka, Corrosion resistant plated steel strip and method for producing same, US Patent 4 877 494, 1989.
[2] Y. Miyoshi, H. Odashima, Y. Shindo, M. Yoshida, T. Kamanaru, Development of Precoated Steel Sheets for Automotive Use, Nippon Steel Technical Report No. 57, (1993), pp. 16–21.
[3] K. Hasegawa, H. Nakamaru, K. Mochizuki, T. Katagiri, N. Morito, S. Kurokawa, Method of producing zink-chromium alloy plated steel sheet with excellent plating adhesiveness,US Patent 5 273 643, 1993.
[4] T. Ichida, Future prospects for electrogalvanized steel Chicago, Illinois, USA, September 1995, Conference Proceedings 'GALVATECH'95' (2018) 359–369.
[5] H. Nakamaru, T. Fujimura, H. Ohnuma, K. Mochizuki, N. Morito, M. Katayama, Corrosion resistant steel sheets improved in corrosion resistance and other characteristics, US Patent 5 510 196, 1996.
[6] M. Nakazawa, A. Takahashi, K. Matsumura, Process for producing zink-chromium alloy-electroplated steel plate, US Patent 5 616 232, 1997.
[7] T. Steck, J. Gerdenitsch, A. Tomandl, W. Achtleiner, J. Faderl, T. Lavric, T. Boiadjieva-Scherzer, H. Kronberger, Zinc-chromium coated steel sheet – properties and production Genova (Italy) June, 8th International Conference on Zinc and Zinc Alloy Coated Steel Sheet Galvatech 2011 (2011) 21–24 Proceedings.
[8] G. Luckeneder, M. Fleischanderl, T. Steck, K.-H. Stellnberger, J. Faderl, S. Schuerz, G. Mori, Coorosion mechanisms and cosmetic corrosion aspects of zinc-aluminium-magnesium and zinc-chromium alloy coated steel strip Genova (Italy) June, 8th International Conference on Zinc and Zinc Alloy Coated Steel Sheet Galvatech 2011 (2011) 21–24 Proceedings..
[9] Ts. Mutafchiev, Corrosion of Metals, Technika Press, Sofia, 1964.
[10] X.G. Zhang, Corrosion and Electrochemistry of Zinc, Plenum Press, New York, 1996.
[11] Tz. Boiadjieva, M. Monev, Chromium alloys, in: B. Franco (Ed.), Chemistry, Production and Application, "Electrodeposition, Composition and Properties of Zn-Cr Alloy Coatings", Nova publishers, New York, 2014, pp. 1–41.
[12] Tz. Boiadjieva-Scherzer, H. Kronberger, G. Fafilek, M. Monev, Hydrogen evolution reaction on electrodeposited Zn-Cr alloy coatings, J. Electroanal. Chem. 783 (2016) 68–75.
[13] Tz. Boiadjieva, K. Petrov, G. Raichevski, M. Monev, Changes in composition and structure of electrodeposited Zn-Cr alloy coatings resulting in corrosion treatment, Trans. IMF 84 (6) (2006) 313–319.
[14] Tz. Boiadjieva, D. Kovacheva, K. Petrov, S. Hardcastle, M. Monev, Effect of anodic treatment on the composition and structure of electrodeposited Zn-Cr alloy coatings, Corros. Sci. 46 (3) (2004) 681–695.
[15] M. Pourbaix, Atlas of Electrochemical Equilibria in Aqueous Solutions, Pergamon Press, London, 1966.
[16] Tz. Boiadjieva, D. Kovacheva, K. Petrov, S. Hardcastle, A. Sklyarov, M. Monev, Electrodeposition, composition and structure of Zn-Cr alloys, J. Appl. Electrochem. 34 (3) (2004) 315–321.
[17] H. Itani, J. Duchoslav, M. Arndt, T. Steck, J. Gerdenitsch, J. Faderl, K. Preis, W. Winkler, D. Stifter, X-ray photoelectron and scanning Auger electron spectroscopy study of electrodeposited ZnCr coatings on steel, Anal. Bioanal. Chem. 402 (1) (2012), http://dx.doi.org/10.1007/s00216-012-5788-y.
[18] D. Rafaja, Deconvolution versus convolution – a comparison for materials with concentration gradient, Mater. Struct. 7 (2) (2000) 43–51.